Korean J. Chem. Eng., 35(3), 744-749 (2018)
DOI: 10.1007/s11814-017-0320-x

pISSN: 0256-1115
eISSN: 1975-7220

Characteristics of photocatalytic decomposition of individual and binary mixture vapors of some VOCs by a cylindrical UV reactor with helically installed TiO_2-coated perforated planes

Jin-Woo Jeon*, Dong-Hwan Lee, Yong Sun Won*, and Min-Gyu Lee*,†**

*Department of Chemical Engineering, Pukyong National University, Busan 48547, Korea
**Department of Chemistry, Dong Eui University, Busan 47340, Korea
(*Received 14 September 2017 • accepted 20 November 2017*)

Abstract−The photocatalytic decomposition characteristics of individual and binary vapors of benzene, toluene, and ethylbenzene by a UV reactor were studied. The reactor was custom-designed to have a synergistic effect of photochemical oxidation by ozone generated by $UV_{254+185\,nm}$ lamps and photocatalytic oxidation by TiO_2 photocatalyst whose surface area was almost doubled by helically inserted TiO_2-coated perforated planes. The removal efficiencies of individual vapors of benzene, toluene, and ethylbenzene generally increased in proportion to the relative humidity and oxygen supply. The photocatalytic decomposition kinetics of individual vapors, as well as binary vapors consisting of benzene-toluene, benzene-ethylbenzene, and toluene-ethylbenzene, followed the Langmuir-Hinshelwood (L-H) equation quite well. Maximum elimination capacities of individual vapors were 560 g/m^3·day, 630 g/m^3·day, and 1,024 g/m^3·day for benzene, toluene, and ethylbenzene, respectively. In view of mutual impact for the photocatalytic decomposition of binary vapors, the reaction rate of the target component was more influenced by the presence of the counter component with lower bond dissociation energy.

Keywords: Photocatalytic Decomposition, Benzene, Toluene, Ethylbenzene, UV Reactor, Ozone, TiO_2

INTRODUCTION

Rapid urbanization and industrialization accompanied by the increase of fossil fuel usage have led to the problem of volatile organic compound (VOC) emission [1]. VOCs not only damage the central nervous system (CNS) but also cause cancer and respiratory disease in humans with inhalation and prolonged exposure [2].

As measures to remove VOCs in effluent gas, there have been condensation [3], adsorption [4], biofiltration [5], catalytic combustion [6], and UV catalytic decomposition [7]. However, condensation is a high thermal budget technology especially for dilute effluent gas. Adsorption also has disadvantages of the efficiency decrease with high moisture content and troublesome disposal of used adsorbent materials despite its high VOC removal efficiency with low cost [8]. Catalytic combustion requires high installation/operation costs and causes secondary pollution involving NOx during its high temperature operation [9]. On the other hand, UV photocatalytic decomposition is environmentally friendly where VOCs are decomposed very efficiently just under UV illumination by photocatalysts, and economical thanks to its low operational cost, and has good operability at atmospheric pressure and room temperature. The research on this technology has been carried out in three ways; (1) increasing the charging amount of photocatalysts in the reactor [10], (2) applying additional strong oxidants such as hydrogen peroxide (H_2O_2) and ozone [11,12], and (3) studying the kinetics and mechanism for the elimination of individual VOC components [13-15].

Ku et al. [16] and Korologos et al. [15] used reactor walls coated with photocatalysts. Verbruggen et al. [10] charged glass-beads coated with photocatalysts to increase the coating area of photocatalysts for improving the efficiency of ethylene removal, but UV illumination hardly reached to the inside. Meanwhile, Dionysiou et al. [17] and Vorontsov [12] reported improving the efficiency of VOC removal by applying H_2O_2 vapor. Shen and Ku [18], Pengyi et al. [19], and Yoa et al. [20] attained the same effect by using an ozone generator. As an alternative to the ozone generator, $UV_{254+185\,nm}$ lamps (with a maximum emission at 254 nm and a minor emission (<5%) at 185 nm) were verified to be efficient for the VOC removal by Feiyan et al. [21], Jeong et al. [11], and Huang and Leung [22]. We have also reported the efficient toluene removal by a custom-designed UV reactor having the synergistic effect of photochemical oxidation by ozone generated by $UV_{254+185\,nm}$ lamps and photocatalytic oxidation by TiO_2 photocatalysts whose surface area was almost doubled by helically inserted TiO_2-coated perforated planes [7].

Strini et al. [13] and Ku et al. [16] investigated the elimination characteristics of individual VOC components, and kinetic studies for individual VOC gases were also done by Bouzaza et al. [23] and Korologos et al. [15]. Wen et al. [2] and Quici et al. [14] conducted mechanistic studies for individual benzene and toluene as well. However, the effluent gas from industry contains multiple VOC components, and the removal characteristics of mixture gases by a UV reactor would be different from those of individual VOC components. Mutual impacts among VOC components have to

†To whom correspondence should be addressed.
E-mail: mglee@pknu.ac.kr

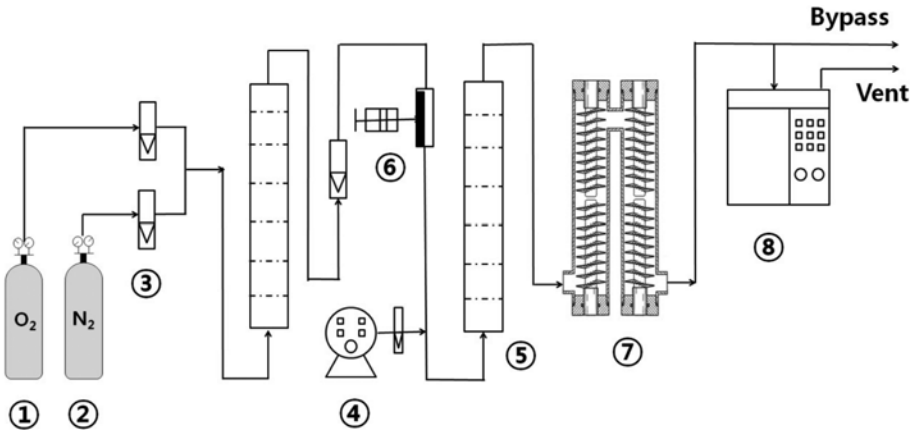

Fig. 1. Schematic diagram of experimental apparatus.
① O_2 gas cylinder ② N_2 gas cylinder ③ Flow meters ④ humidifier ⑤ Mixing chamber ⑥ Syringe pump ⑦ UV photocatalytic reactor with perforated planes ⑧ Gas chromatography

be considered.

In this study, we investigated the removal characteristics of individual benzene, toluene, and ethylbenzene by using our custom-designed reactor, where TiO_2-coated perforated planes are helically installed to increase the coating area of photocatalysts and simultaneously $UV_{254+185\,nm}$ and $UV_{254\,nm}$ lamps are placed in the front and rear half of the reactor, respectively, to produce ozone as an additional oxidant and decrease the emission of hazardous residual ozone [7]. The effect of relative humidity and oxygen supply was also examined on the photocatalytic decomposition of individual components. Then, our study was extended to evaluate mutual impacts during the decomposition of binary mixture vapors.

MATERIALS AND METHODS

We employed almost the same experimental setup as in our previous study [7]. As shown in Fig. 1, a syringe pump (Cole Parmer International, p074901-10) injects liquid benzene, toluene, ethylbenzene, and their binary liquid mixtures to be vaporized by mixed carrier gas, flown out from O_2 and N_2 gas cylinders (high-purity with water concentration <20 ppmv). The mixture gases are fed to a mixing chamber for further mixing with water vapor generated from an electric humidifier (Hanil, UH645) to adjust the humidity. The oxygen supply is controlled by the regulation of O_2 and N_2 gas flow rates, and the humidity is controlled by the regulation of water vapor flow rate. Vaporized benzene, toluene, ethylbenzene, and their binary mixture vapors with their humidity and oxygen supply regulated are then introduced in the bottom part of our custom-designed UV reactor. Our custom-designed UV photocatalytic reactor had TiO_2-coated perforated planes helically installed inside the reactor [7]. The whole reactor system (⑦ in Fig. 1) consisted of two connected identical cylindrical reactors whose diameter and length are 3.5 cm and 60 cm, respectively. Then, two 16 W $UV_{254+185\,nm}$ lamps (with a maximum emission at 254 nm and a minor emission (<5%) at 185 nm) and two 16 W $UV_{254\,nm}$ lamps were installed in the first and second reactors, respectively. Perforated stainless steel planes coated with TiO_2 of 1 μm thickness were inserted helically in the reactors, wound 36 times around the UV lamps. The surface area of TiO_2-coated perforated planes is 1,520 cm^2, while TiO_2-coated reactor walls have a surface area of 1,280 cm^2. The outlet concentrations of benzene, toluene, and ethylbenzene were measured by a GC (Donam, DS-6200) mounted with a flame ionization detector (FID). The temperatures of the oven, injector, and detector in the GC analyzer were 100 °C, 200 °C, and 200 °C, respectively, and the flow rate ratio of $N_2 : H_2$: air was 30 : 30 : 300.

RESULTS AND DISCUSSION

1. Effect of Relative Humidity on the Removal of Individual Vapor

Fig. 2 shows the removal efficiencies of individual vapors (benzene, toluene, and ethylbenzene) by changing relative humidity. The removal efficiencies of benzene, toluene, and ethylbenzene are 41%, 42%, and 50%, respectively, at the relative humidity of 15%. The removal efficiency generally increases with the relative humid-

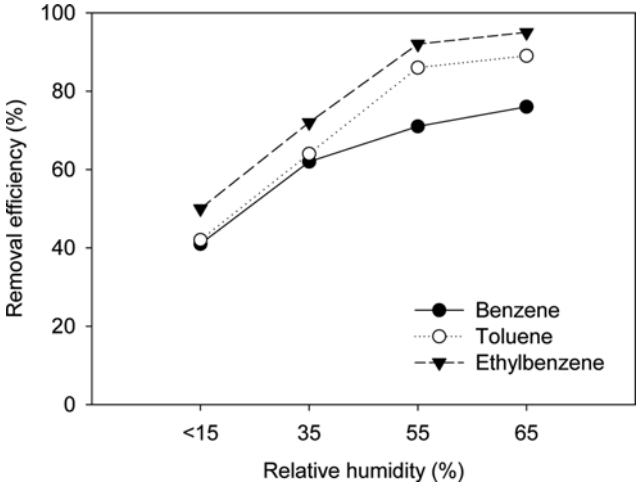

Fig. 2. Effect of relative humidity on the removal efficiencies of benzene, toluene, and ethyl benzene (initial concentration= 50 ppmv, linear velocity=3.9 m/min).

ity − 62%, 71%, and 76% for benzene, 64%, 86%, and 89% for toluene, 72%, 92%, and 95% for ethylbenzene at the relative humidity of 35%, 55%, and 65%, respectively. Similar results were reported by Peral and Ollis [24], and Hennezel et al. [25]. Generally, the presence of water in a photocatalytic reaction would promote the formation of hydroxyl radicals (·OH), a strong oxidant, on the surface of photocatalysts, and hydroxyl radicals contribute to the decomposition of aromatic compounds [26]. Therefore, the removal efficiency of benzene, toluene, and ethylbenzene was increased because a large amount of hydroxyl radicals were produced as the relative humidity increased. However, the tendency was somewhat released at the relative humidity of above 55%. It is considered that when the water vapor concentration reaches a certain value, the removal efficiency no longer increases because water vapors compete with VOC compounds for the adsorption sites on the TiO_2 surface, eventually to hinder VOC adsorption.

2. Effect of Oxygen Concentration on the Removal of Individual Vapor

To examine the effect of oxygen on the photocatalytic conversion of individual vapors (benzene, toluene, and ethylbenzene), photocatalytic degradation tests were carried out at an atmosphere of synthetic air comprising pure nitrogen and pure oxygen. Fig. 3 shows the removal efficiencies of individual vapors (benzene, toluene, and ethylbenzene) by changing oxygen concentration. The removal efficiency of benzene, toluene, and ethylbenzene is less than 21% when pure nitrogen is used. Then, the increase of oxygen concentration to 21% and 100% (pure oxygen) enhances the removal efficiencies; 41% and 47% for benzene, 42% and 50% for toluene, 50% and 55% for ethylbenzene. The existence of oxygen enhances the photocatalytic decomposition of target vapors because oxygen as an electron acceptor forms hydroxyl radicals [27]. However, even if the oxygen concentration increased from 21% to 100%, the removal efficiency was not increased significantly. It is considered that oxygen acts as an electron acceptor to prevent recombination of electrons and holes, so that it would not have a great influence on the removal efficiency above a certain oxygen concentration due to the presence of sufficiently formed electron acceptors [28].

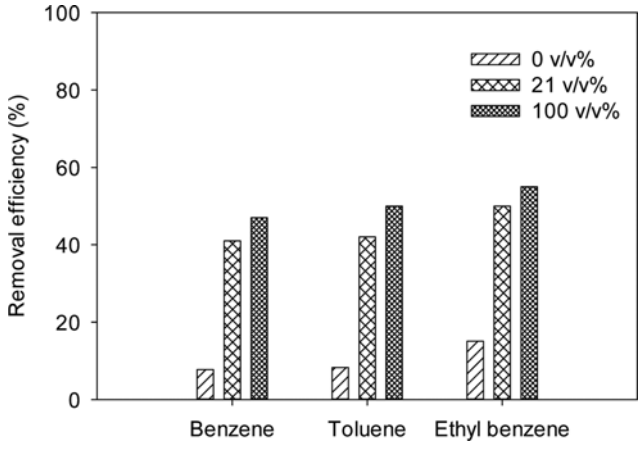

Fig. 3. Effect of oxygen concentration on the removal efficiencies of benzene, toluene, and ethylbenzene (initial concentration= 50 ppmv, linear velocity=3.9 m/min).

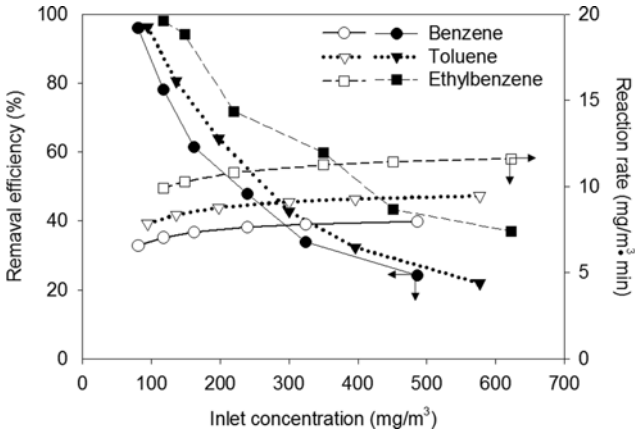

Fig. 4. Effect of inlet concentration on the removal efficiencies of benzene, toluene, and ethylbenzene (linear velocity=3.9 m/min, relative humidity=35%).

3. Effect of Inlet Concentration on the Removal of Individual Vapor

Fig. 4 shows the changes of removal efficiency and reaction rate of individual vapors according to their inlet concentration. As shown, the removal efficiency decreases with the increase of inlet concentration, but the reaction rate increases. The decrease of removal efficiency is because the active sites of the TiO_2 surface become saturated as the inlet concentration of the reactant increases [29]. On the other hand, the increases of the reaction rates are thought to be caused by the increase of the concentration difference (in other words, the increase of the driving force for mass transfer). At the same inlet concentration, the order of removal efficiency is ethylbenzene>toluene>benzene. In fact, the order of removal efficiency corresponds to the order of reaction rates in Fig. 4. The destruction of VOCs by photocatalytic reactions occurs as a result of reactions with hydroxyl radicals formed when the TiO_2 is UV-irradiated. Therefore, the reaction rates are practically related to the bond dissociation energies of VOCs [30]. The bond dissociation energies of benzene, toluene and ethylbenzene are known as 112.9 (C_6H_5-H), 88.5 ($C_6H_5CH_2$-H) and 85.4 kcal/mol ($C_6H_5C_2H_4$-H), respectively [31]. When benzene, toluene, and ethylbenzene gain potential energy above their bond dissociation energies, they dissociate into radicals of $\cdot C_6H_5$, $\cdot C_6H_5CH_2$, and $\cdot C_6H_5C_2H_4$, respectively. Therefore, the removal efficiency of ethylbenzene, having the lowest bond dissociation energy among them, would be the highest because it dissociates to its radical and reacts with hydroxyl radical more easily than benzene or toluene. On the other hand, benzene with the highest bond dissociation energy would show the lowest removal efficiency. The reaction rates of benzene, toluene and ethylbenzene were 6.59-7.99, 7.86-9.46, and 9.90-11.61 mg/m^3·min, respectively. As anticipated, the reaction rate (or the removal efficiency) was reciprocally proportional to the bond dissociation energy. This is also in accordance with the result reported by Jolly et al. [30] for several classes of organic compounds.

The UV photocatalytic oxidation is expressed by the following Langmuir-Hinshelwood (L-H) equation [15].

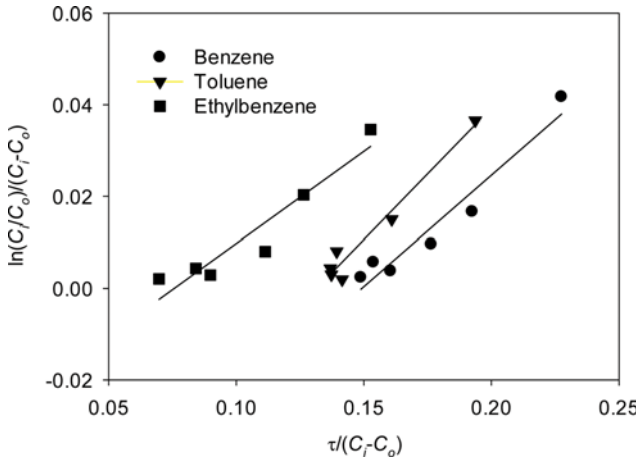

Fig. 5. Regression of experimental results with the L-H kinetic model.

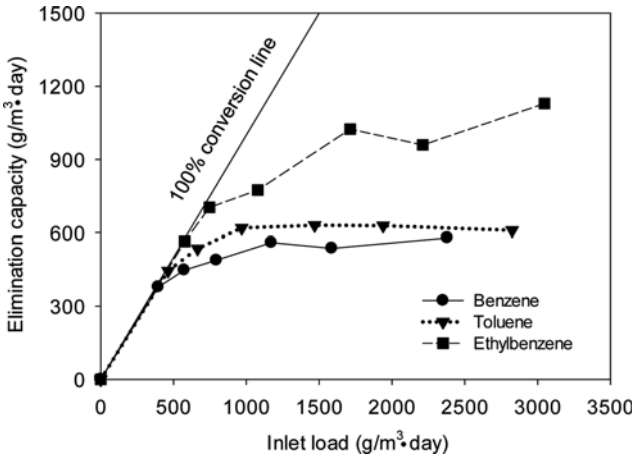

Fig. 6. Elimination capacities of benzene, toluene, and ethylbenzene with increasing inlet load (linear velocity=3.9 m/min, relative humidity=35%).

Table 1. L-H model parameters obtained from the regression of experimental results

VOC	kK (1/min)	K (m^3/mg)×10^2	k (mg/m^3·min)	r^2
Benzene	0.485	7.23	6.71	0.938
Toluene	0.574	7.55	7.60	0.962
Ethylbenzene	0.402	3.04	13.22	0.902

$$r = \frac{kKC}{1+KC} \quad (1)$$

where r is the reaction rate in mg/m^3·min, k is the rate constant for photocatalysis in mg/m^3·min, K is the rate constant for adsorption in m^3/mg, and C is the concentration of the VOC in mg/m^3.

By substituting Eq. (1) into a mass balance on a plug flow reactor, the following expression is obtained.

$$\frac{\ln(C_i/C_o)}{C_i - C_o} = kK\frac{\tau}{C_i - C_o} - K \quad (2)$$

where C_i is the inlet concentration in mg/m^3, C_o is the outlet concentration in mg/m^3, and τ is the retention time in minute.

Fig. 5 plots the results by applying Eq. (1) into the data in Fig. 4, and the calculated parameters are summarized in Table 1. The L-H kinetic model gave decent fits with r^2=0.938, 0.962, and 0.902 for benzene, toluene, and ethylbenzene, respectively. Interestingly, the order of the reaction rate constant has a reciprocal consistency with the order of removal efficiency: 6.71 mg/m^3·min for benzene <7.60 mg/m^3·min for toluene <13.22 mg/m^3·min for ethylbenzene.

4. Elimination Capacity of Individual Vapor with Inlet Load

The elimination capacity with respect to the inlet load is one of the essential parameters in designing and operating a UV photocatalytic reactor system. The inlet load and maximum elimination capacity of benzene, toluene, and ethylbenzene in our system were thus obtained by the followings.

$$\text{Inlet load} = \frac{C_i Q}{V} \quad (3)$$

Table 2. Maximum elimination capacities of benzene, toluene, and ethylbenzene in our study compared with other studies

VOC	Inlet load (g/m^3·day)	Maximum elimination capacity (g/m^3·day)	References
Benzene	521	89	Ku et al. [16]
	36	17	Korologos et al. [15]
	106	44	Wang et al. [33]
	84	77	Jeong et al. [11]
	318	32	Boulamanti et al. [32]
	1,170	560	This study
Toluene	503	116	Ku et al. [16]
	104	41	Korologos et al. [15]
	222	156	Pengyi et al. [19]
	393	216	Jeong et al. [11]
	239	72	Boulamanti et al. [32]
	968	630	This study
Ethylbenzene	119	66	Korologos et al. [15]
	508	152	Boulamanti et al. [32]
	1,710	1,024	This study

$$\text{Elimination capacity} = \frac{(C_i - C_0)Q}{V} \quad (4)$$

where C_i is the inlet concentration in mg/m^3, C_o is outlet toluene concentration in mg/m^3, V is reactor volume in m^3, and Q is flow rate in m^3/min.

Fig. 6 plots the elimination capacities of individual vapors (benzene, toluene, and ethylbenzene) with changing the inlet load by applying Eqs. (3) and (4), and Table 2 summarizes maximum elimination capacities of individual vapors from other studies compared to our results. For references, the maximum elimination capacities of UV/TiO_2 processes with simple TiO_2-coated reactor walls were 17-89 g/m^3·day at the inlet load of 36-521 g/m^3·day for benzene,

41-116 g/m^3·day at the inlet load of 104-503 g/m^3·day for toluene, and 66 g/m^3·day at the inlet load of 119 g/m^3·day for ethylbenzene [15,16]. The maximum elimination capacities of O_3/UV/TiO_2 processes with the ozone effect added to simple UV/TiO_2 processes were 32-77 g/m^3·day at the inlet load of 84-318 g/m^3·day for benzene, 72-216 g/m^3·day at the inlet load of 222-393 g/m^3·day for toluene, and 152 g/m^3·day at the inlet load of 508 g/m^3·day for ethylbenzene [11,19,32]. Meanwhile, we obtained maximum elimination capacities of 560 g/m^3·day at 1,170 g/m^3·day for benzene, 630 g/m^3·day at 968 g/m^3·day for benzene, and 1,024 g/m^3·day at 1,710 g/m^3·day for benzene. Those are superior to the values of other studies by about 2-10 times. Again, the increase of TiO_2 coating area by installing TiO_2-coated perforated planes inside the reactor combined with additional photochemical oxidation by ozone generated by $UV_{254+185\,nm}$ lamps explains these results.

5. Removal Characteristics of Binary Mixture Vapors

In the photocatalytic decomposition of mixed vapors, the photocatalytic reaction rate of the target vapor would be affected by the existence of other vapors. The influence of the component B (counter component) on the reaction rate of the component A (target component) in the mixture relative to the photocatalytic reaction of the individual component A can be described as follows [34]:

$$\text{Impact factor} = \frac{\text{Reaction rate of the specified component in mixture}}{\text{Reaction rate of individual component}} \quad (5)$$

If the impact factor is between 0 and 1, component B depresses the reaction rate of component A. If the impact factor is equal to 1, component B does not affect the reaction rate of component A. If the impact factor is greater than 1, component B enhances the reaction rate of component A.

To know the interrelationship between the target VOCs, the photocatalytic reaction characteristics of binary mixture vapors are examined. Fig. 7 shows the change of elimination capacities for binary mixture vapors (benzene & toluene, benzene & ethylbenzene, and toluene & ethylbenzene) when the inlet load of one of the components is set to 94 mg/m^3 and the inlet load of the other component is increased.

Table 3 summarizes maximum elimination capacities, reaction rate, and impact factors obtained from the data in Fig. 7. As shown in Table 3, the maximum elimination capacity of benzene is 560 g/m^3·day, but the value is decreased to 236 g/m^3·day in the presence of toluene and to 157 g/m^3·day in the presence of ethylbenzene. While the reaction rate of benzene is 6.59-7.83 mg/m^2·min, the value is decreased to 1.41-2.83 g/m^3·day in the presence of toluene and to 0.61-2.35 g/m^3·day in the presence of ethylbenzene. On the other hand, the impact factor of benzene with toluene is 0.21-0.36, higher than 0.09-0.30 with ethylbenzene, indicating that the decomposition of benzene is more depressed by the presence of ethylbenzene. For other combinations, the decomposition of toluene is more depressed by the presence of ethylbenzene than benzene, and the decomposition of ethylbenzene is more depressed by toluene than benzene. From these results, the reaction rate of the target component was more influenced by the presence of the counter component with lower bond dissociation energy in the photocatalytic decomposition of mixture vapors.

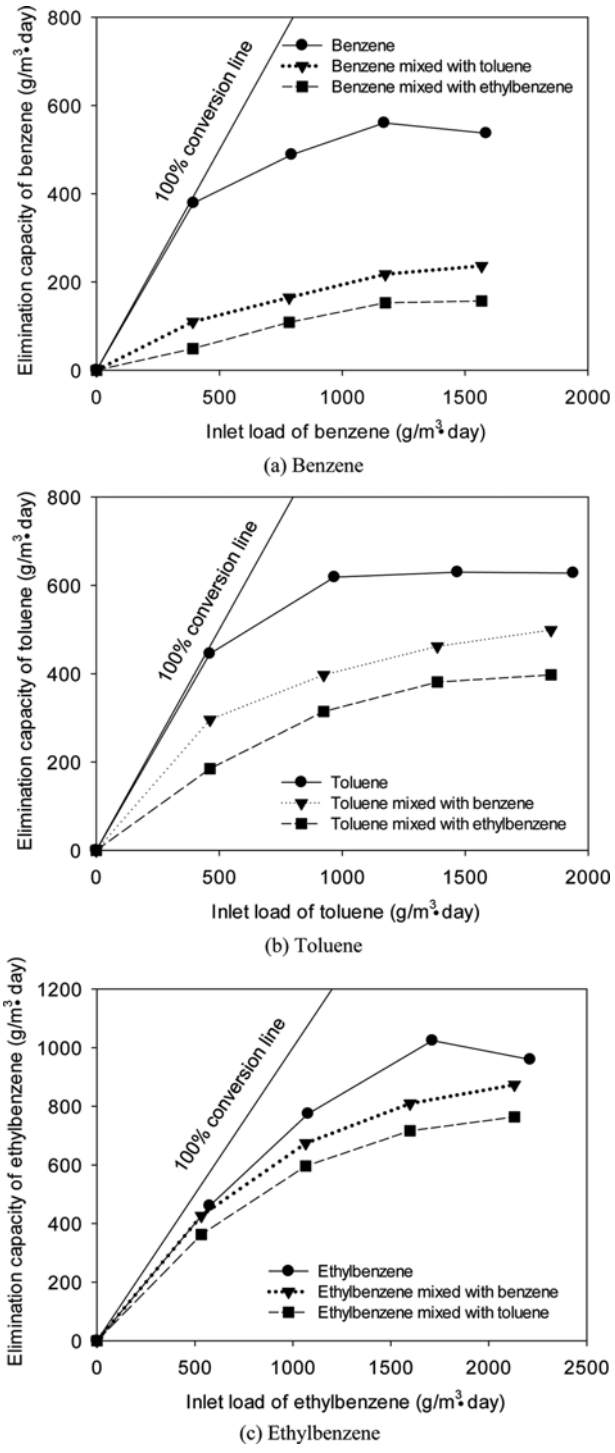

Fig. 7. Comparison of the elimination capacities for single vapors and their binary mixture vapors (linear velocity=3.9 m/min, relative humidity=35%).

CONCLUSIONS

We investigated the removal characteristics of benzene, toluene, and ethylbenzene in our custom-designed reactor in which TiO_2-coated perforated planes are helically installed inside to increase TiO_2 coating area and simultaneously $UV_{254+185\,nm}$ lamps are placed

Table 3. Comparison of maximum elimination capacities, reaction rate, and impact factors obtained for single vapors and their binary mixture vapors

VOC	Maximum elimination capacity ($g/m^3 \cdot day$)				r ($mg/m^2 \cdot min$)				Impact factor		
	S	M_{B+T}	M_{B+EB}	M_{T+EB}	S	M_{B+T}	M_{B+EB}	M_{T+EB}	M_{B+T}	M_{B+EB}	M_{T+EB}
Benzene	560	236	157		6.59-7.83	1.41-2.83	0.61-2.35		0.21-0.36	0.09-0.30	
Toluene	630	499		398	7.86-9.29	5.00-8.14		3.42-8.14	0.64-0.88		0.43-0.88
Ethylbenzene	1024		874	764	9.90-11.44		7.16-10.68	5.77-9.70		0.72-0.93	0.58-0.85

S: single component
M_{B+T}: binary vapor of benzene and toluene
M_{B+EB}: binary vapor of benzene and ethylbenzene
M_{T+EB}: binary vapor of toluene and ethylbenzene

to gain an additional effect by ozone generation. The maximum elimination capacities of individual vapors were 560 $g/m^3 \cdot day$ at the inlet load of 1,170 $g/m^3 \cdot day$ for benzene, 630 $g/m^3 \cdot day$ at 968 $g/m^3 \cdot day$ for benzene, and 1,024 $g/m^3 \cdot day$ at 1,710 $g/m^3 \cdot day$ for benzene. Then, the increase of relative humidity and oxygen supply in carrier gas generally enhanced the removal efficiency because of the generation of more hydroxyl radicals and additional ozone, respectively. In the photocatalytic decomposition of binary mixture vapors, the decomposition of benzene was more depressed by the presence of ethylbenzene than toluene, while toluene was more depressed by the presence of ethylbenzene than benzene, and ethylbenzene was more depressed by toluene than benzene.

ACKNOWLEDGEMENTS

This work was supported by the Korea Institute of Energy Technology Evaluation and Planning (KETEP) and the Ministry of Trade, Industry & Energy (MOTIE) of the Republic of Korea (No. 20174010201460).

REFERENCES

1. F. Gironi and V. Piemonte, *Chem. Eng. J.*, **172**, 671 (2011).
2. WHO, World Health Organization Guidelines for Drinking Water Quality, *World Health Organization*, Geneva, Switzerland (2004).
3. A. Hamad and M. E. Fayed, *Chem. Eng. Res. Des.*, **82**, 895 (2004).
4. S. W. Lee, J. K. Cheon, H. J. Park and M. G. Lee, *Korean J. Chem. Eng.*, **25**, 1154 (2008).
5. J. K. Kim, S. K. Kam and M. G. Lee, *Int. J. Environ. Pollut.*, **39**, 264 (2009).
6. J. S. Cho, M. W. Ryoo, K. S. Song, J. H. Lee and S. K. Kang, *Korean J. Chem. Eng.*, **16**, 478 (1999).
7. Y. S. Won, J.-W. Jeon, D.-H. Lee and M. G. Lee, *J. Chem. Eng. Jpn.*, **50**, 289 (2017).
8. K. Urashima and J. S. Chang, *IEEE Transactions on Dielectrics and Electrical Insulation*, **7**, 602 (2000).
9. C. Y. Cha and C. T. Carlisle, *J. Air Waste Manage. Assoc.*, **51**, 1628 (2011).
10. S. W. Verbruggen, S. Ribbens, T. Tytgat, B. Hauchecorne, M. Smits, V. Meynen, P. Cool, J. A. Martens and S. Lenaerts, *Chem. Eng. J.*, **174**, 318 (2011).
11. J. Y. Jeong, K. Sekiguchi, W. K. Lee and K. Sakamoto, *J. Photochem. Photobiol. A: Chem.*, **169**, 279 (2005).
12. A. V. Vorontsov, *Catal. Commun.*, **8**, 2100 (2007).
13. A. Strini, S. Cassese and L. Schiavi, *Appl. Catal. B: Environ.*, **61**, 90 (2005).
14. N. Quici, M. L. Vera, H. Choi, G. L. Puma, D. D. Dionysiou, M. I. Litter and H. Destaillats, *Appl. Catal. B: Environ.*, **95**, 312 (2010).
15. C. A. Korologos, C. J. Philippopoulos and S. G. Poulopoulos, *Atmos. Environ.*, **45**, 7089 (2011).
16. Y. Ku, J. S. Chen and H. W. Chen, *J. Air Waste Manage. Assoc.*, **57**, 279 (2007).
17. D. D. Dionysiou, M. T. Suidan, I. Baudin and J. M. Laine, *Appl. Catal. B: Environ.*, **50**, 259 (2004).
18. Y. S. Shen and Y. Ku, *Chemosphere*, **46**, 101 (2002).
19. Z. Pengyi, L. Fuyan, Y. Gang, C. Qing and Z. Wanpeng, *J. Photochem. Photobiol. A: Chem.*, **156**, 189 (2003).
20. S.-J. Yoa, Y.-S. Cho and J.-H. Kim, *Korean J. Chem. Eng.*, **22**, 364 (2005).
21. C. Feiyan, S. O. Pehkonen and M. B. Ray, *Water Res.*, **36**, 4203 (2002).
22. H. B. Huang and D. Y. C. Leung, *J. Environ. Eng.*, **137**, 996 (2011).
23. A. Bouzaza, C. Vallet and A. Laplanche, *J. Photochem. Photobiol. A: Chem.*, **177**, 212 (2006).
24. J. Peral and D. F. Ollis, *J. Catal.*, **136**, 544 (1992).
25. O. d'Hennezel, P. Pichat and D. F. Ollis, *J. Photochem. Photobiol. A: Chem.*, **118**, 197 (1998).
26. K. C. Jung and S. C. Hong, *J. Korean Ind. Eng. Chem.*, **14**, 671 (2003).
27. S. B. Kim, H. T. Hwang and S. C. Hong, *Chemosphere*, **48**, 437 (2002).
28. D. Y. Shin and K. N. Kim, *J. Korean Ceramic Soc.*, **45**, 43 (2008).
29. J. Shang, W. Li and Y. Zhu, *J. Mol. Catal. A: Chem.*, **202**, 187 (2003).
30. G. S. Jolly, G. Paraskevopoulos and D. L. Singleton, *Int. J. Chem. Kinet.*, **17**, 1 (1985).
31. Y. R. Luo, *Handbook of bond dissociation energies in organic compounds*, CRC Press, 392 (2003).
32. A. K. Boulamanti, C. A. korologos and C. J. Philippopoulos, *Atmos. Environ.*, **42**, 7844 (2008).
33. W. Wang, L. W. Chiang and Y. Ku, *J. Hazard. Mater.*, **101**, 133 (2003).
34. Y. P. Zhang, R. Yang, Q. J. Xu and J. H. Mo, *J. Air Waste Manage. Assoc.*, **57**, 94 (2007).